Report
P-19-06
August 2020

EBS TF – THM modelling

Water transport in pellets-filled slots – laboratory tests and task descriptions

Mattias Åkesson
Reza Goudarzi
Lennart Börgesson

SVENSK KÄRNBRÄNSLEHANTERING AB

SWEDISH NUCLEAR FUEL
AND WASTE MANAGEMENT CO

Box 3091, SE-169 03 Solna
Phone +46 8 459 84 00
skb.se

SVENSK KÄRNBRÄNSLEHANTERING

ISSN 1651-4416
SKB P-19-06
ID 1896522
August 2020

EBS TF – THM modelling

Water transport in pellets-filled slots – laboratory tests and task descriptions

Mattias Åkesson, Svensk Kärnbränslehantering AB

Reza Goudarzi, Lennart Börgesson
Clay Technology AB

Abstract

This report presents the experimental work performed with the purpose to be used within EBS Taskforce “Task 10 Water transport in pellets-filled slots”. The aim of this task was to investigate the ability of models (existing or new) to simulate water transport at different test conditions. Two subtasks have addressed two test types: A) 1D-tests with water freely available (water uptake tests), and C) 1D-tests with water redistribution in a temperature gradient. Tests were performed with two different pellets materials: extruded Asha NW BFL-L and roller compacted MX-80.

The methodology, the equipment and the results for both test types are described and discussed in this report. In addition, task descriptions for the two subtasks are defined together with a specification of the requested model results. Finally, the report presents the methodology, equipment and results of tests in which the air permeability of roller compacted MX-80 pellets was investigated.

Sammanfattning

Denna rapport presenterar ett experimentellt arbete som utförts i syfte att användas inom samarbetsprojektet ”Task force on Engineered Barrier Systems” och modelleringsuppgiften Task 10 ”Vattentransport i pelletsfyllda spalter”. Målet med denna uppgift var att undersöka olika materialmodellers (befintliga eller nya) förmåga att simulera vattentransport under olika testförhållanden. Två deluppgifter har inriktats mot två testtyper: A) 1D-tester med fri tillgång på vatten (vattenupptagsförsök), och C) 1D-tester med fuktomfördelning i en temperaturgradient. Testerna utfördes med två olika pelletsmaterial: extruderad Asha NW BFL-L, och rullkompakterad MX-80.

Metodologin, utrustningen och resultaten för de båda testtyperna beskrivs och diskuteras i denna rapport. Dessutom definieras uppgiftsbeskrivningar för de båda deluppgifterna tillsammans med en specifikation av efterfrågade modellresultat. Slutligen presenteras metodologi, utrustning och resultat för tester i vilka luft-permeabiliteten för MX-80 pellets undersöktes.

Contents

1 Introduction

There is a need to have material models for pellets-filled slots that can be used in water uptake simulations of the buffer material in deposition holes and of the backfill material in deposition tunnels. In simulations made today (e.g. Sellin et al. 2017), where the actual bentonite geometry with blocks and pellets are modelled, too simple assumptions about the behaviour of the pellet filling must usually be used and the result of these simulations cannot reflect the actual wetting behaviour. This is especially obvious at inflow rates of 10^{-2} l/min or lower from a fracture. The hydro-mechanical behaviour is complicated and differs a lot at different inflow rates. In addition, many of the deposition holes are foreseen to be very dry, which calls for better understanding of the temperature-driven water transport.

In the project EVA (Consequences of water inflow and early water uptake in deposition holes) large progress in the understanding of many processes related to water inflow into deposition holes (or tunnels) has been attained but this has also led to an insight into how complicated these processes are and the incapability of the present models to simulate the inflow pattern in pellet fillings (Börgesson et al. 2015). A pellet filling has a double structure (with gas-filled pores both inside and between the individual pellets) that changes its properties as the degree of water saturation increases and in addition it cannot withstand water pressure but will suffer from piping and other even more unpleasant processes (e.g. water-filled pockets).

In order to remedy this shortcoming a modelling task, denoted *Water transport in pellets-filled slots* was defined within the framework of EBS Taskforce during 2016. The aim of the task was to formulate new models or (if available) use existing models for water transport in pellet fillings and to calibrate and check their ability to model water transport at different boundary and inflow conditions and at different temperature situations. This report presents a number of basic laboratory tests performed to be used within this modelling task.

Four different subtasks were originally proposed:

- Subtask A. 1D-tests with water freely available (water uptake tests).
- Subtask B. Constant water inflow rate from point inflow.
- Subtask C. 1D-tests with water redistribution in a temperature gradient.
- Subtask D. 1D-tests with water freely available in a temperature gradient.

These subtasks were planned to be based on experimental data from four corresponding test types. However, due to limited resources, only tests within two of the subtasks (A and C) could be performed and included in the task description, which was distributed in September 2016. This description was subsequently complemented with results for two additional Subtask C tests, which were finalized and distributed in March 2019. A task description for subtask B was distributed in June 2018. This was based on experimental work, financed by Posiva Oy, which will be published elsewhere.

The pellets types used in the tests are described in Chapter 2. The type A tests and the type C tests are presented in Chapter 3 and Chapter 4, respectively. A description of the different subtasks is presented in Chapter 5. A few supplementary air permeability tests are described in Chapter 6, and some concluding remarks are finally given in Chapter 7.

2 Description of bentonite pellets

Two types of pellets manufactured from MX-80 and Asha bentonites were used in the tests. The pellets were sieved in order to remove all fines.

2.1 Extruded 6 mm rods (Asha NW BFL-L)

This bentonite is produced by Ashapura Minechem Co. The bentonite is quarried in the Kutch area on the northwest coast of India. The bentonite is sodium dominated. The pellets made of this material have been manufactured at Äspö HRL (batches of the raw material were delivered to SKB 2010 and 2012).

This pellets type is manufactured by extrusion i.e. the bentonite is pressed through a hole-matrix, which results in pellets shaped as rods with varying length. The data of the pellets and the material is described in the following reports: Sandén et al. (2014, 2016), Sandén and Jensen (2016), and Johannesson et al. (2008). Basic data of the pellets:

- Montmorillonite content ~70 %
- Particle density $\rho_s = 2\,920$ kg/m^3
- Water content $w = 15.6$ %
- Individual pellet properties:
  - Dry density $\rho_d = 1\,924$ kg/m^3
- Bulk properties after installation (measured before tests):
  - Dry density $\rho_d = 958$ kg/m^3

The actual values in the tests described below were slightly different in some cases.

The appearance of this pellets-type is illustrated in Figure 2-1.

Figure 2-1. *Extruded 6 mm rod shaped extruded pellets (Asha).*

2.2 Compacted pillows (MX-80-11)

These roller compacted pillow shaped pellets are made of MX-80 and manufactured using a roller compaction technique where the material is compacted between two counter-rotating wheels with cut-outs. The pellets were manufactured by HOSOKAWA Bepex GmbH in Germany.

The data of the pellets and the material is the following (Andersson and Sandén 2012):

- Montmorillonite content ~ 80 %
- Particle density $\rho_s = 2\,780$ kg/m^3
- Water content w = 15.0 %
- Individual pellet properties:
  - Dry density $\rho_d = 1\,841$ kg/m^3
- Bulk properties after installation (measured before tests):
  - Dry density $\rho_d = 953$ kg/m^3

The actual values in the tests described below were slightly different in some cases.

The appearance of this pellets-type is illustrated in Figure 2-2.

Figure 2-2. *Compacted pillow shaped roller compacted pellets (MX-80-11).*

3 Test type A

3.1 Test description

These tests have yielded information about the water transport when the hydraulic properties of the pellet filling, rather than the boundary condition, control the inflow rate. Plexiglas cylinders, 50 cm long and with an inner diameter of 10 cm were used for the tests. Tap water was available in a filter in the bottom. The top of the cylinder was sealed with a lid, which in turn was connected to a flexible balloon with the purpose of avoiding a gas pressure build-up.

Measurements of the relative humidity (RH) were made in three points in one of the tests, and the cumulative water uptake (q) was measured in all tests (Figure 3-1). The tests were run for different times and the water content profile was measured at the end of each test. The two types of pellets described in Chapter 2 were used in the tests. Table 3-1 shows the original test matrix. Two sets of test equipment were used due to the long duration of some tests.

The filter in the bottom of the tube was connected to a reservoir with a water surface fixed at a defined level above the filter. The reason for this was to ensure that proper contact was reached between the water and the pellets filling. The constant head was upheld with a peristaltic pump which continuously supplied water from an external reservoir (Figure 3-2). A head of 1–2 cm (corresponding to 0.1–0.2 kPa) was used in the short-term tests, whereas a head of 10 cm (1 kPa) was used in the long-time tests Ar3 and Ae3.

The tests set-up is shown in Figure 3-2. The RH transducers were located 3, 8 and 15.5 cm above the filter. The water uptake (q) was measured by weighing the external reservoir for each test regularly.

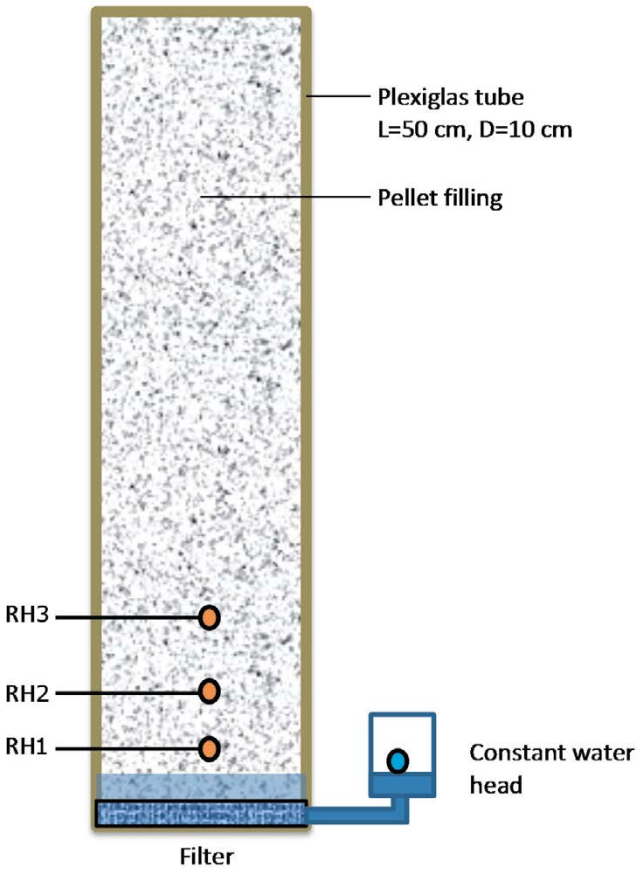

Figure 3-1. *Test arrangement for test type A.*

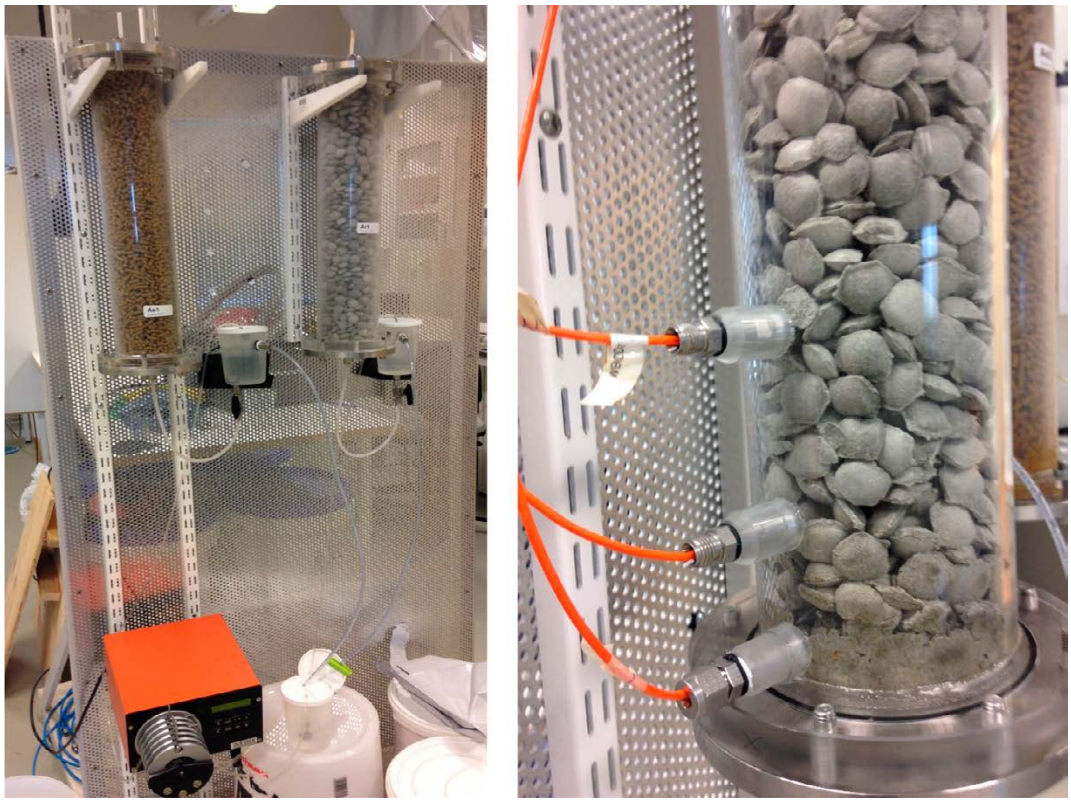

Figure 3-2. *Test set-up for the water uptake tests (Test type A). Left photo: Extruded pellets in the left tube and roller compacted in the right tube. The peristaltic pump and the two external reservoirs can be seen beneath the test set-up. Right photo: Close up of the bottom part of a test with MX-80 pellets with installed RH-transducers.*

Table 3-1. Original test matrix for test type A.

Test	Pellet type	Duration	Measurement
Ar1	RC MX-80	5 days	q
Ar2	RC MX-80	30 days	q
Ar3	RC MX-80	200 days	RH, q
Ae1	Ex Asha	5 days	q
Ae2	Ex Asha	30 days	q
Ae3	Ex Asha	200 days	RH, q

3.2 Results

The original test matrix was largely followed. One additional test performed earlier (denoted Ar3b) was also included. Table 3-2 shows the actual test matrix.

After termination of the tests, the water content was determined as a function of the distance from the inlet filter. Results of the water content profile are thus available at three times for each pellet type together with the results from the earlier test. Figure 3-3 and Figure 3-4 show the measured water content profiles for the two pellet types.

The large initial water inflow was caused by water flowing into the pellets just after connecting the filter to the water level in the jar. The larger initial inflow observed for tests Ar3 and Ae3 was thus caused by the higher water pressure that was applied in those tests.

Figure 3-5 shows the evolution of the measured water uptake in all tests. No water uptake was measured in the earlier test Ar3b. Figure 3-6 shows the RH evolution in test Ar3.

Table 3-2. Final actual test matrix for test type A.

Test	Pellet type	Duration	Measurement	Water pressure
Ar1	RC MX-80	5 days (120 h)	q	0.1 kPa
Ar2	RC MX-80	30 days (720 h)	q	0.2 kPa
Ar3	RC MX-80	203 days (4 872 h)	RH, q	1.0 kPa
Ar3b	RC MX-80	181 days (4 344 h)	-	-
Ae1	Ex Asha	5 days	q	0.2 kPa
Ae2	Ex Asha	30 days	q	0.2 kPa
Ae3	Ex Asha	202 days (4 848 h)	q	1.0 kPa

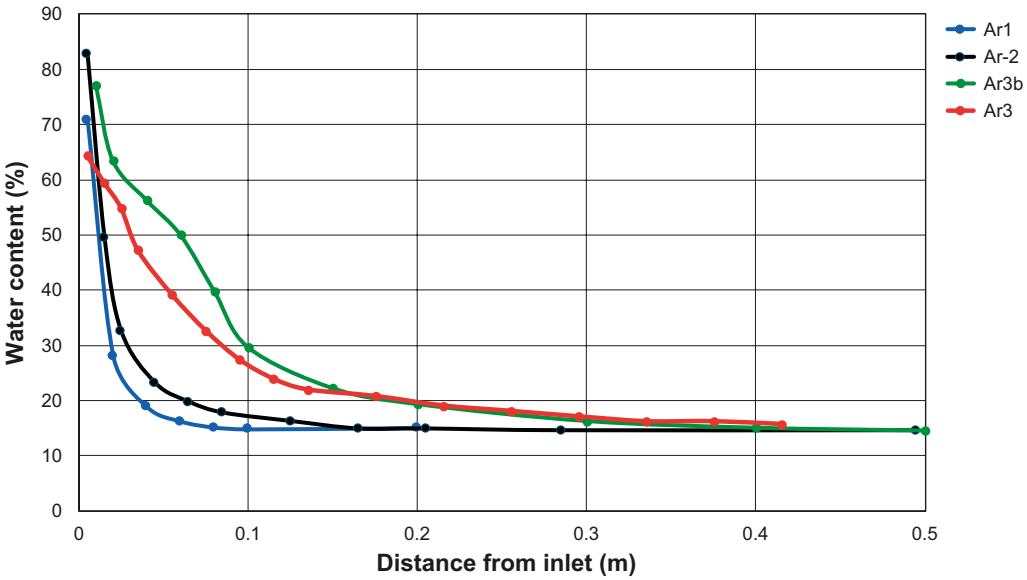

Figure 3-3. Water content profiles at the end of test for tests on roller compacted MX-80 pellets.

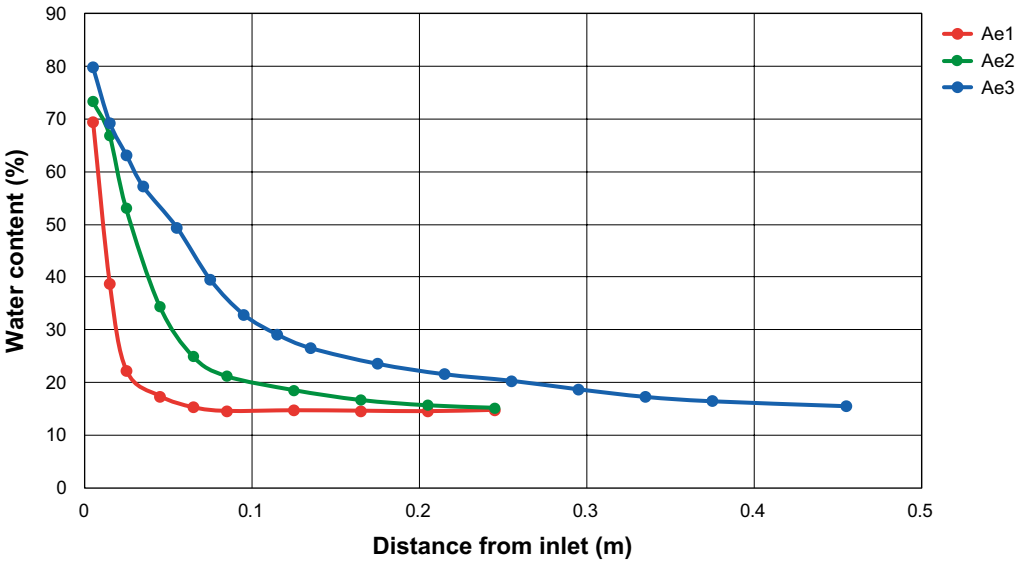

Figure 3-4. Water content profiles at the end of test for tests on extruded Asha pellets.

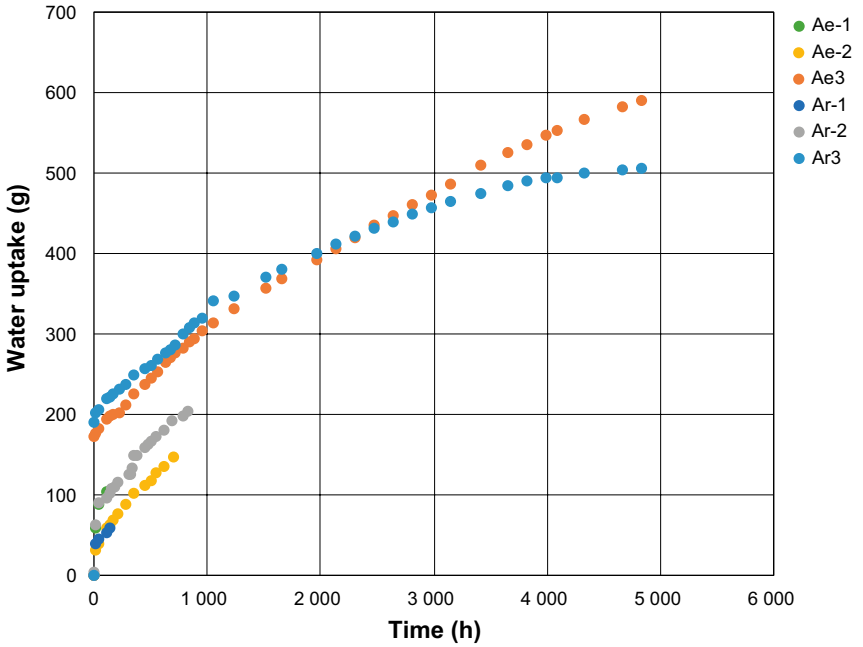

Figure 3-5. Water uptake versus time.

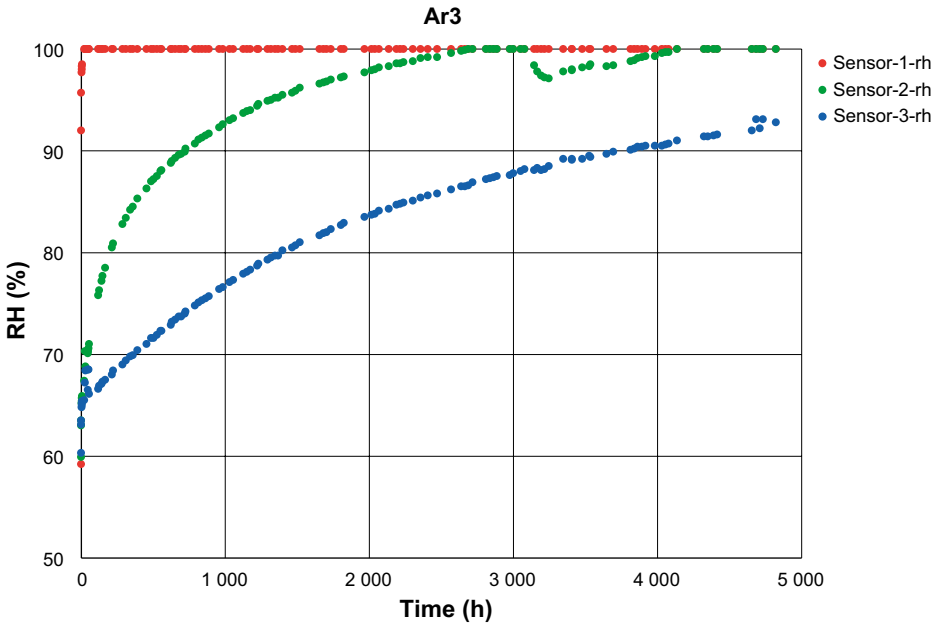

Figure 3-6. RH versus time in test Ar3. Sensor 1, 2 and 3 were located 3, 8 and 15.5 cm from the water inlet, respectively.

3.3 Discussion

Three evaluations of the consistency of different data sets are presented below regarding: i) the water content profiles and the water uptake; ii) the water content and the RH; and iii) the initial water uptake and the boundary pressure.

Water content increase vs water uptake

The final measured water uptake was compared with a calculated water uptake (Δm_w) which in turn was based on the water content profile measured at the end of the test:

$$\Delta m_w = \rho_d \cdot A \cdot (\sum w_i \cdot l_i - w^{init} \cdot L) \qquad (3\text{-}1)$$

where ρ_d is the dry density, A is the section area, L is the length of the equipment, w^{init} is the initial water content, and w_i and l_i are the water content and the length, respectively, of each sample i. A compilation of measured and calculated water uptake values for the Ar3 and Ae3 tests are shown in Table 3-3. The differences between these values are significant, and the most likely explanation for this was that the measured water uptake data was influenced by different types of evaporation and leakage (the average rate of mass loss would be less than 1 gram per day). The calculated water uptake may appear to correspond with the measured water uptake *after the initial* uptake seen in Figure 3-5, and this may therefore suggest that the initial uptake did not enter the pellets. However, several observations indicate that this is coincidental: i) a rapid increase of the measured RH, especially at 3 cm distance from the water inlet; ii) the observation that this RH-sensor was covered by liquid water shortly after the start of the test; and iii) a general relationship between the initial water uptake and the boundary pressure (see below), and these observations therefore support the notion that the measured water uptake data was influenced by evaporation and leakage.

Water content vs RH

RH measurements were performed in one of the Type A tests: Ar3. The initial general RH level and the final values for the two sensors located most distant from the water inlet were put in relation with the water content in the pellets adjacent to the sensors at the time of the sensor reading. This set of in-situ retention data (Figure 3-7) can be compared with independently determined water retention curves for two different initial water contents: 17 % (Dueck 2004) and 10 % (Dueck and Nilsson 2010). The overall agreement between these data sets illustrates the accuracy of the used RH sensors.

Table 3-3. Measured and calculated water uptake data.

Test	Water uptake (meas, g)	Water uptake (calc, g)	Difference (g)
Ar3	507	317	190
Ae3	591	436	155

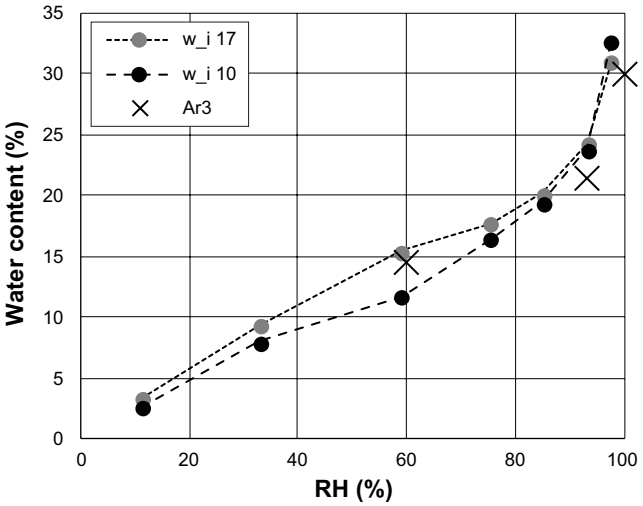

Figure 3-7. *In-situ water retention data (X) and independent water retention data from literature (●).*

Initial water uptake vs boundary pressure

The initial water uptake corresponds to the height (h) if the measured water mass (m_w) fills all gas-filled pore space within this height:

$$h = \frac{m_w}{n \cdot (1 - S_0) \cdot A \cdot \rho_w} \quad (3\text{-}2)$$

where n is the porosity, S_0 is the initial saturation degree, A is the section area and ρ_w is the density of water. An initial water mass of 200 grams corresponds to ~5 cm while 50 gram corresponds to ~1 cm (assuming $n \approx 0.67$ and $S_0 \approx 0.22$). This means that the lower value of the initial water uptake shown in Figure 3-5 appears to reflect the water pressures shown in Table 3-2 accurately. The higher value (200 g) corresponds to a water head approximately half the value of the stated water pressure (1.0 kPa). This may possibly be caused by sealing of the pellets during the initial filling.

Method development

The dimension of the test geometry has a large impact on the timescale of the investigated processes, and the used test equipment with a length of 0.5 m has implied very long test times. In order to obtain as wide-ranging information about the investigated processes as possible within a certain time frame, it would probably be more optimal to decrease the test dimension, however without getting close to the spatial resolution which largely is given by the size of the individual pellets.

The used water supply system in which the pressure level was kept constant through continuous pumping may be replaced by a system with a reservoir which simply is monitored by reading the water level. Such a system was used in the BRIE water uptake tests (Fransson et al. 2017). Even if this would imply that the pressure level will vary with a few kPa, this may be of minor importance once the bentonite adjacent to the filter has homogenized. The water level in such a reservoir should therefore be slowly elevated during the initial stage of the experiment.

The possibility that the water uptake in this type of experiment may be influenced by displacements may call for a procedure in which these displacements are quantified. The simple measurements presented in Section 4.3, which were based on a yard stick and a camera, could provide a useful methodology if it would be further developed.

4 Test type C

4.1 Test description

The Type C tests have given basic information about how moisture is redistributed in a temperature gradient. The tests were performed in a 50 cm long Plexiglass cylinder with a diameter of 10 cm, similar to the ones in the type A tests. No free water was however available. Instead, a temperature gradient was applied along the axis of the cylinder, which were thermally insulated, heated at the bottom and cooled at the top. Measurements of RH and temperature were made in all tests (RH and temperature in 5 and 7 points, respectively). Figure 4-1 shows a schematic drawing of the test arrangements. The same test equipment was used for all tests.

The tests were run for different durations. The same two types of pellets were used as in test type A. Table 4-1 shows the original test matrix. Three temperature gradients and three different times were planned, which would yield altogether 18 tests. The redistribution of RH caused by the temperature gradient was much slower than anticipated so the time schedule was changed, and the lower temperature gradients were excluded from the test matrix. Table 4-2 shows the actual test matrix carried through.

Table 4-1. Original test matrix for test type C.

Test	Pellet type	T_1/T_2	Test duration			Measurement
Cr1-Cr3	RC MX-80	70/20	5 h	1 d	5 d	T, RH
Cr4-Cr6	RC MX-80	50/20	5 h	1 d	5 d	T, RH
Cr7-Cr9	RC MX-80	30/20	5 h	1 d	5 d	T, RH
Ce1-Ce3	Ex Asha	70/20	5 h	1 d	5 d	T, RH
Ce4-Ce6	Ex Asha	50/20	5 h	1 d	5 d	T, RH
Ce7-Ce9	Ex Asha	30/20	5 h	1 d	5 d	T, RH

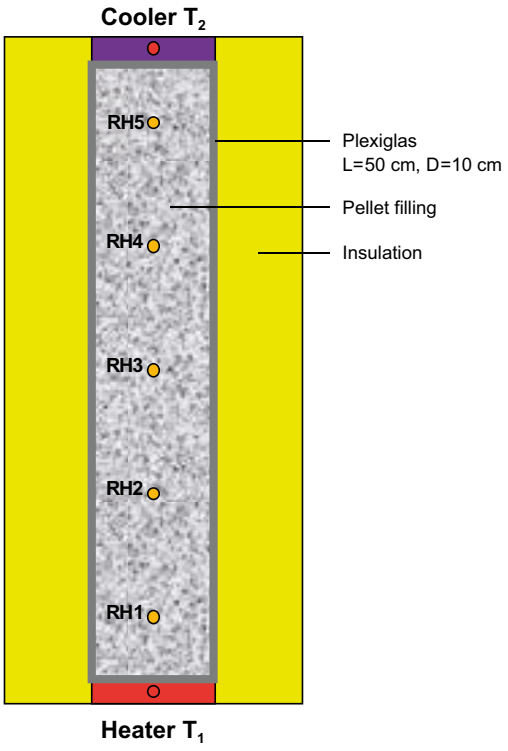

Figure 4-1. *Schematic drawing of the test arrangements. T1 and T2 are the target temperatures of the end plates.*

The temperature on the heater side and the cooled side was in all test 74 and 24 °C, respectively. For the long-term tests, which were run for 90 days or more, the lateral surface of the cylinder was thermally insulated with approximately 14 cm of mineral or glass wool inside a plastic cylinder with a 39 cm inner diameter. In test Cr3d, this was composed of shredded mineral wool (Figure 4-2), while in test Cr3e it was composed of three layers of 45 mm glass wool rolls together with an impervious rubber cover on top (Figure 4-3).

Table 4-2 Final actual test matrix for test type C.

Test	Pellet type	T_1/T_2	Test duration	Measurement	Remarks
Cr1	RC MX-80	74/24	5 h	T, RH	Uncertain
Cr3b	RC MX-80	74/24	7 days (169 h)	T, RH	
Cr3c	RC MX-80	74/24	14 days (331 h)	T, RH	Uncertain
Cr3d	RC MX-80	74/24	91 days	T, RH	
Cr3e	RC MX-80	74/24	364 days	T, RH	
Ce3d	Ex Asha	74/24	90 days (2 161 h)	T, RH	

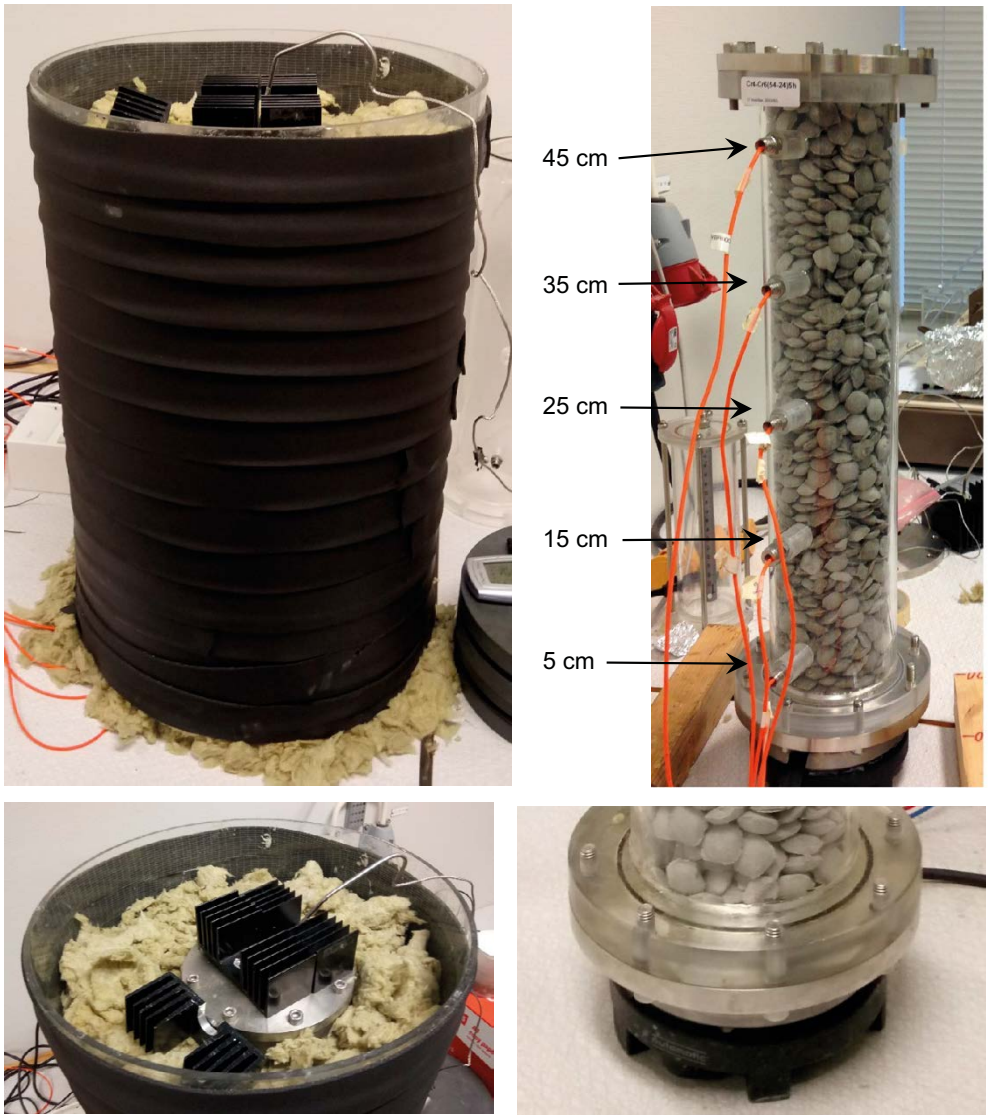

Figure 4-2. *Experimental setup for temperature gradient tests. Pellets-filled test cylinder instrumented with five RH sensors (upper right), outer cover holding mineral wool insulation (upper left), cooling flanges at top end (lower left) and hot plate at lower end (lower right).*

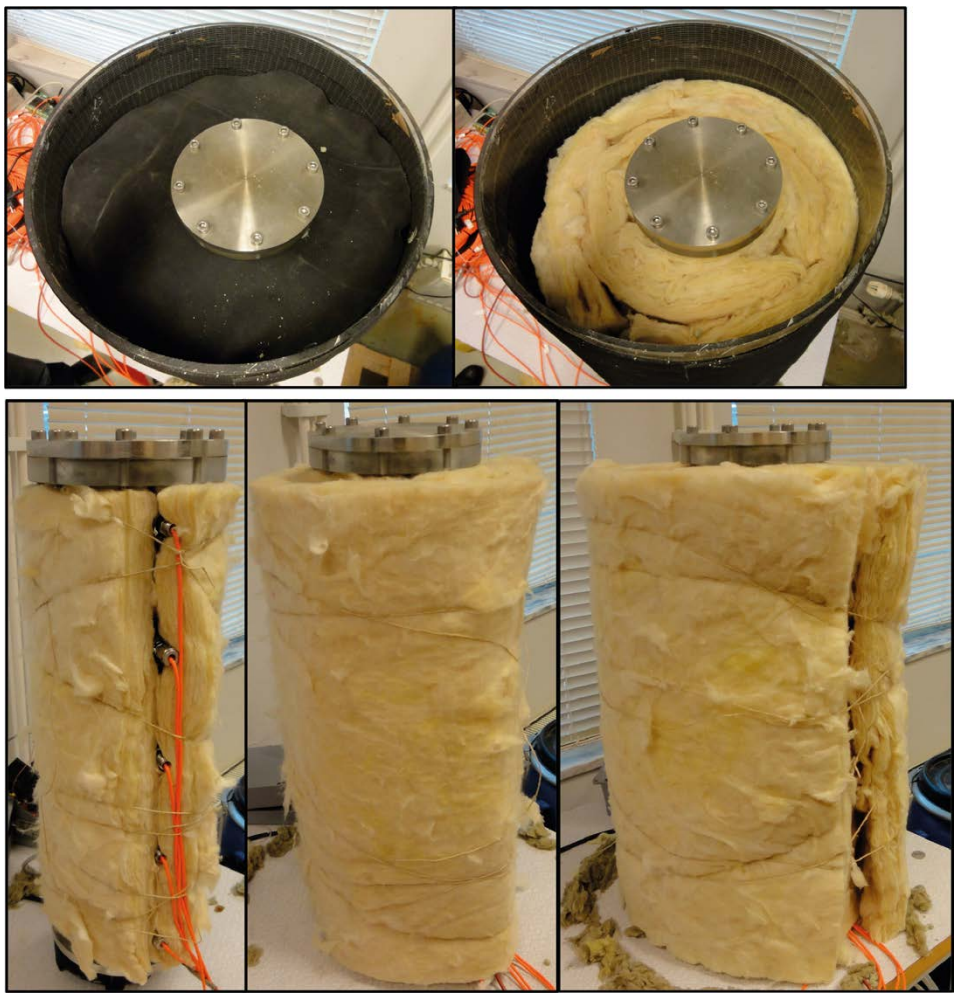

Figure 4-3. *Insulation of test Cr3e. Three layers of glass wool rolls (lower) and enclosing plastic cylinder and rubber cover on top (upper).*

The tube was instrumented with five RH sensors (Aitemin SHT75 V3) which were placed at the distance 5, 15, 25, 35 and 45 cm from the heated bottom plate. Temperature was measured by the RH sensors, on (or inside) the bottom plate, and on the cooling flanges on the top plate. The bottom plate was heated with a temperature controlled hot plate. The cooling was achieved by flanges attached to the top plate in contact with the room atmosphere (Figure 4-2).

The water content distribution was determined after the termination of the test. This was performed by turning the cylinder upside down and by successively removing all material down to specified levels (i.e. 2, 5, 9 etc. cm from above) and by letting the material in each such layer constitute one sample (Figure 4-4). The pellets-filling was in this way divided in 15 or 25 samples for roller-compacted and extruded pellets, respectively. The water content of each sample was determined by drying in an aired oven at 105 °C during 24 hours.

Some of the preliminary initial tests displayed problems with moisture leakage and the thermal insulation. Two preliminary initial tests (Cr1 and Cr3c) were therefore excluded. The most reliable tests were the long-term tests which were run for 90 days or more, i.e. Ce3d with extruded Asha pellets and Cr3d and Cr3e with roller-compacted MX-80.

As mentioned in Chapter 2, the test matrix was complemented with two additional tests. These were performed with the same type of roller compacted MX-80 pellets as used in previous tests. The test denoted Cr3d was run for a duration of 91 days, whereas the test Cr3e was run for 364 days. The initial water content was 14.5 % in both tests. The dry density of the pellets filling was 958 kg/m^3 in test Cr3d and 992 kg/m^3 in test Cr3e.

Figure 4-4. *Sampling of pellets. Opening of lower end of test tube (upper left); removal of material down to a specified level (right); samples in aluminium containers (lower left).*

4.2 Results

Results from the Ce3d test are shown in Figure 4-5 to Figure 4-9. Figure 4-5 and Figure 4-6 show the measured temperature and RH evolution plotted as function of time. Figure 4-7 and Figure 4-8 show the evolution of temperature and RH plotted as functions of the distance from the hot end plate at different times. Figure 4-9 shows the evaluated water content distribution at the end of the test.

Corresponding results from the Cr3d and Cr3e tests are shown in Figure 4-10 to Figure 4-19. Measured evolutions of temperature and RH at sensor positions are shown in Figure 4-10 to Figure 4-13. Profiles of temperature and RH at different times are shown in Figure 4-14 to Figure 4-17. The water content profiles at the end of the tests are shown in Figure 4-18 and Figure 4-19.

Results from the Cr3b test are also rather reliable, although some late improvements of the isolation changed the thermal field. The results from this test are shown in Figure 4-20 to Figure 4-24. Figure 4-24 also shows the water content profiles from tests Cr1 and Cr3c although these results are uncertain.

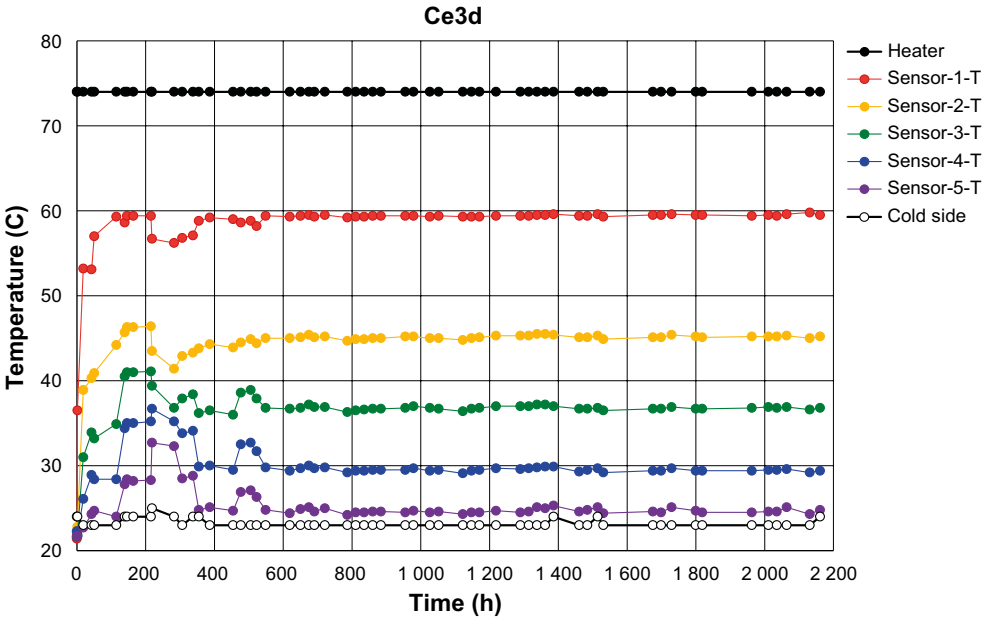

Figure 4-5. *Temperature evolution at sensor positions, heater and cold end in test Ce3d.*

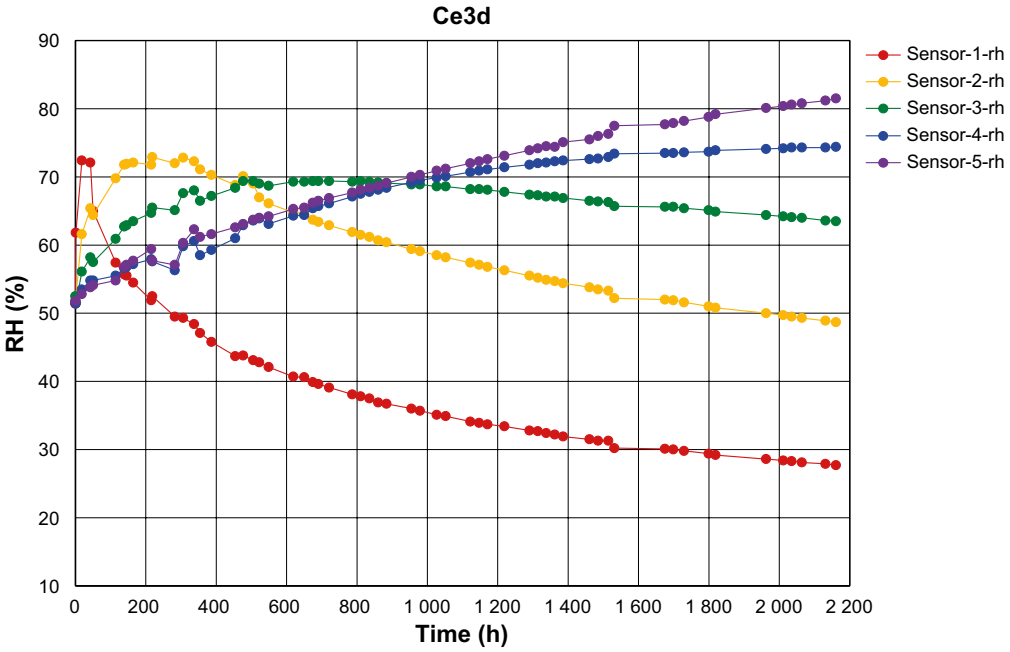

Figure 4-6. *RH evolution at sensor positions in test Ce3d.*

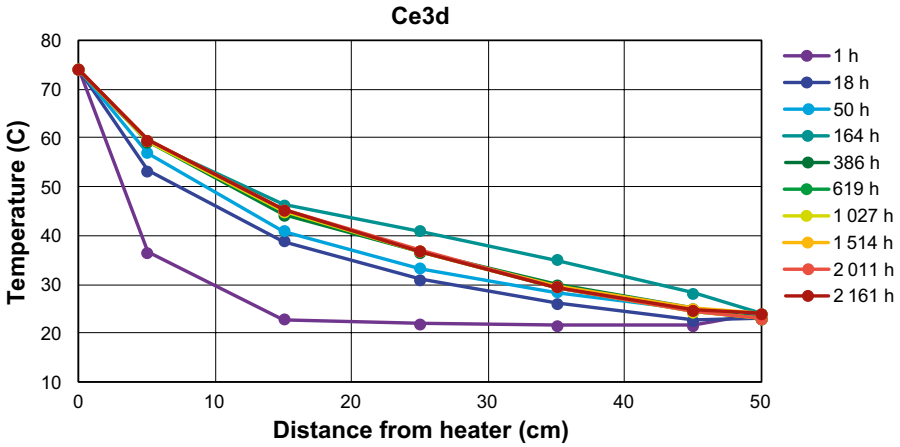

Figure 4-7. *Temperature profiles at different times (hours) in test Ce3d.*

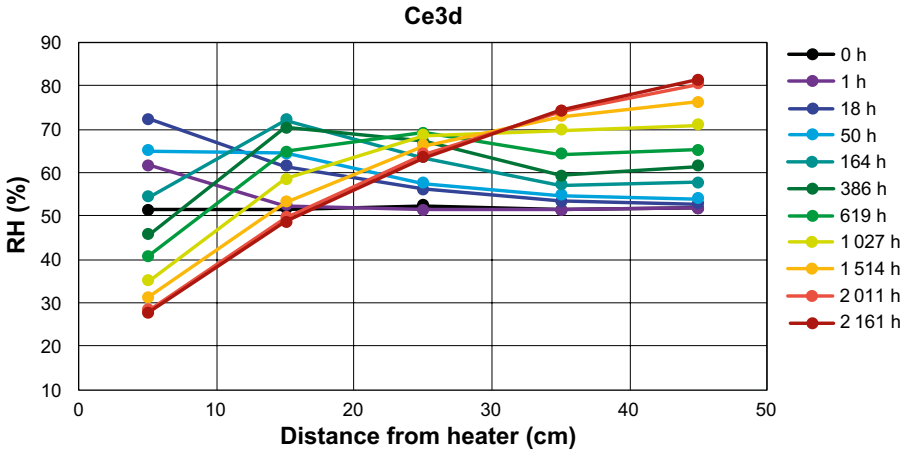

Figure 4-8. *RH profiles at different times (hours) in test Ce3d.*

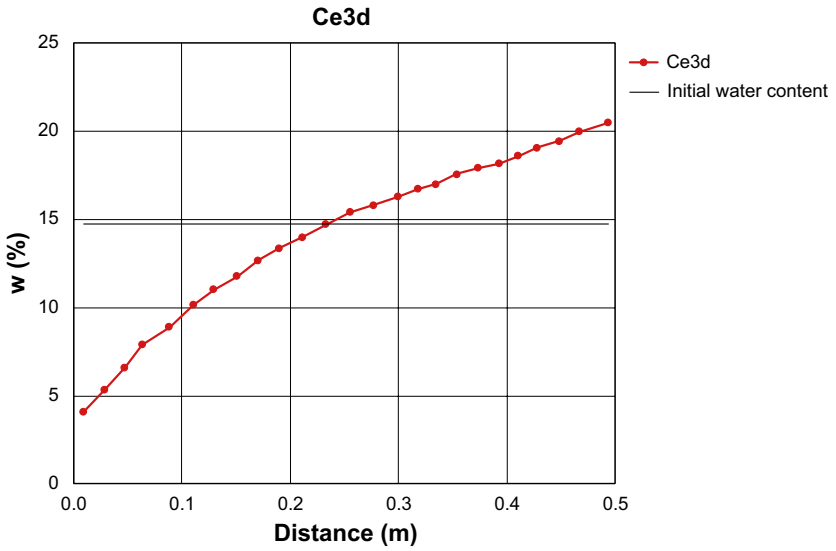

Figure 4-9. *Water content profile at the end of test Ce3d (2 161 hours).*

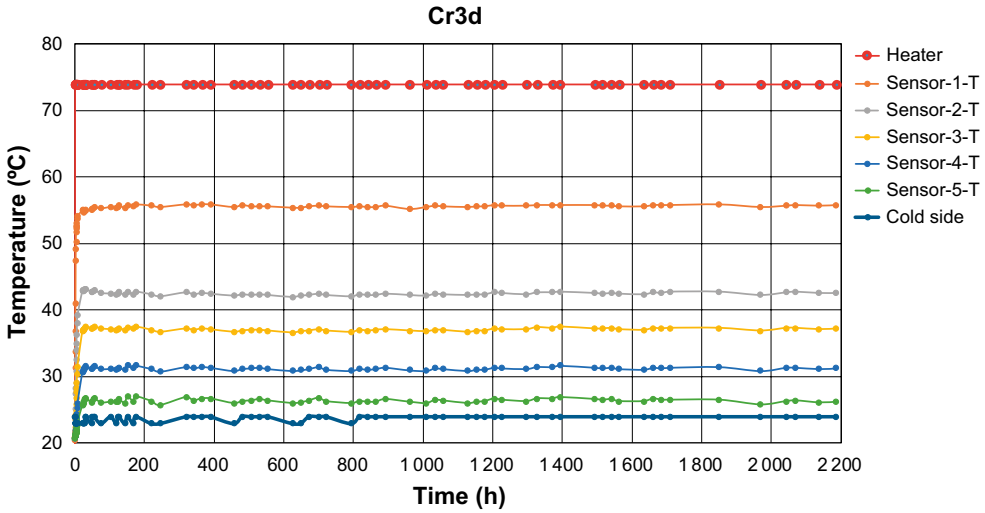

Figure 4-10. *Temperature evolution at sensor positions, heater and cold end in test Cr3d.*

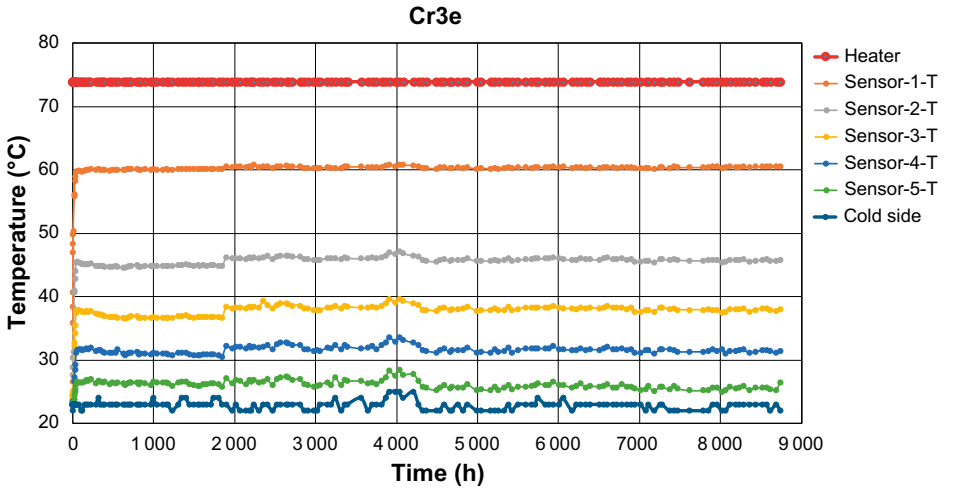

Figure 4-11. *Temperature evolution at sensor positions, heater and cold end in test Cr3e.*

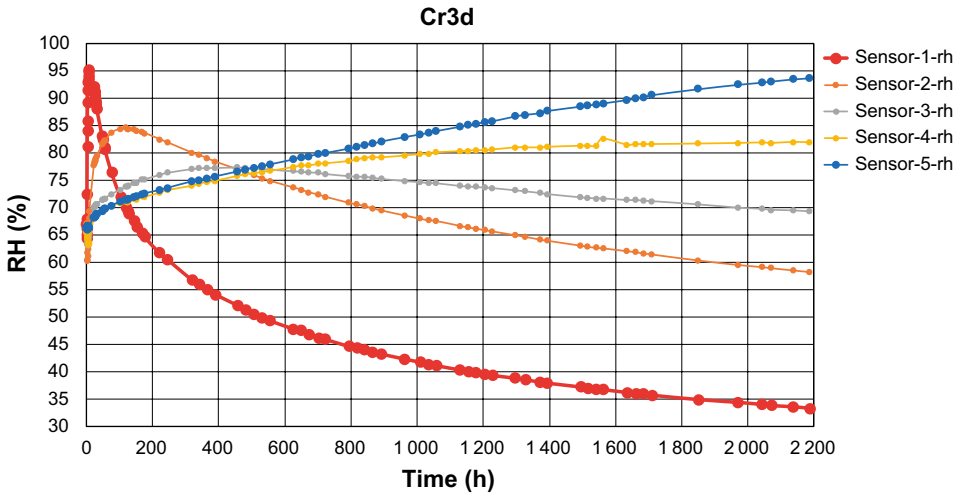

Figure 4-12. *RH evolution at sensor positions in test Cr3d.*

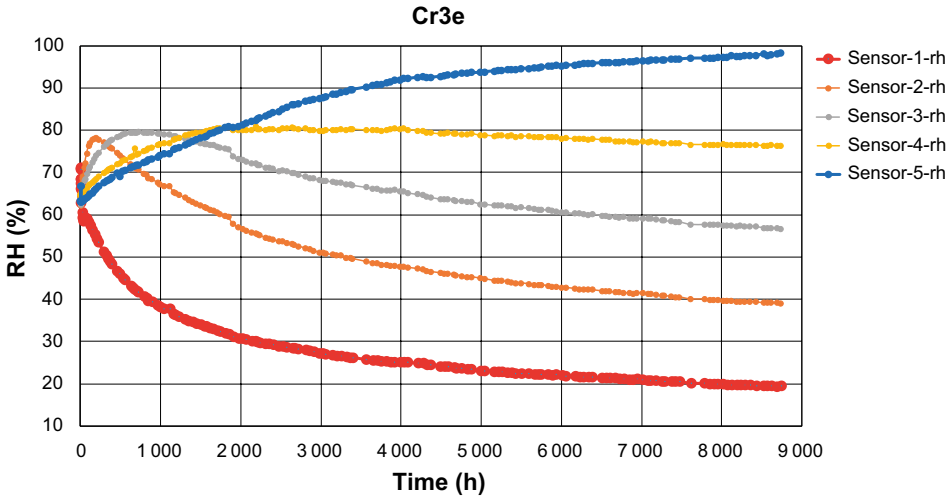

Figure 4-13. *RH evolution at sensor positions in test Cr3e.*

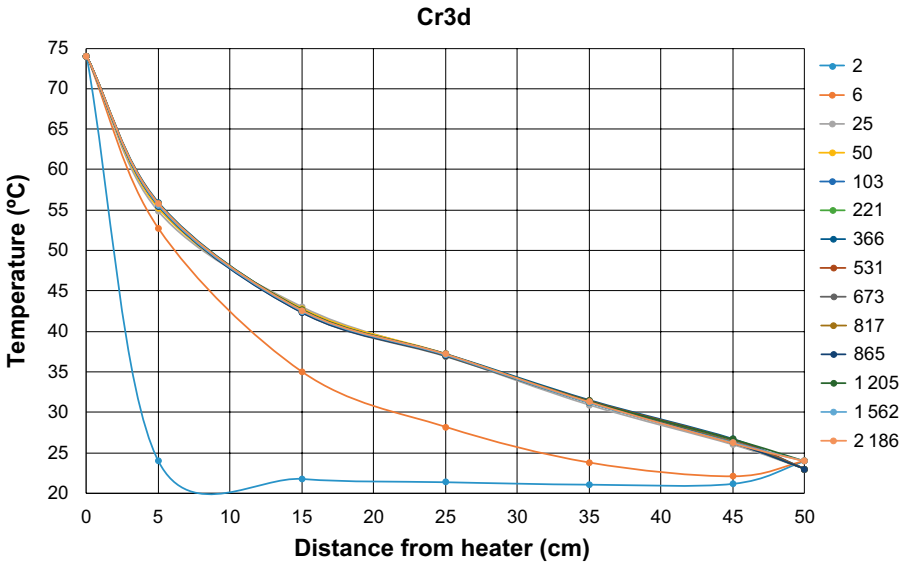

Figure 4-14. *Temperature profiles at different times (hours) in test Cr3d.*

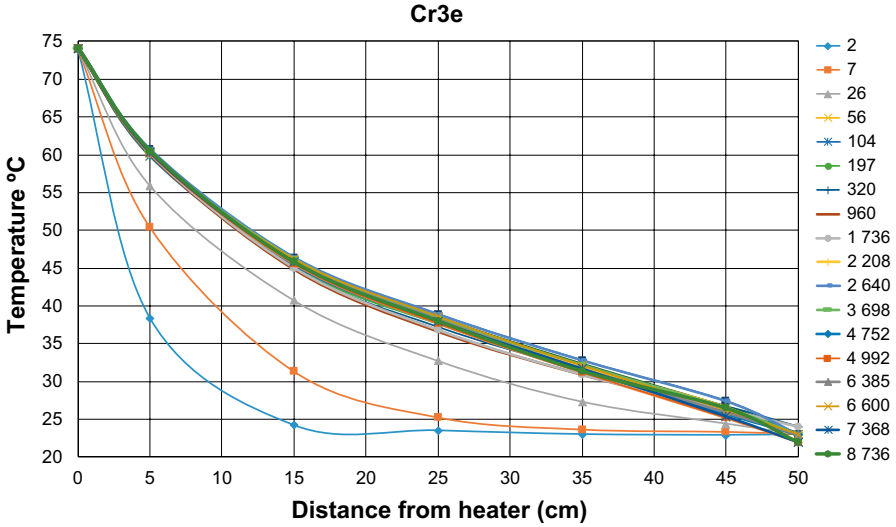

Figure 4-15. *Temperature profiles at different times (hours) in test Cr3e.*

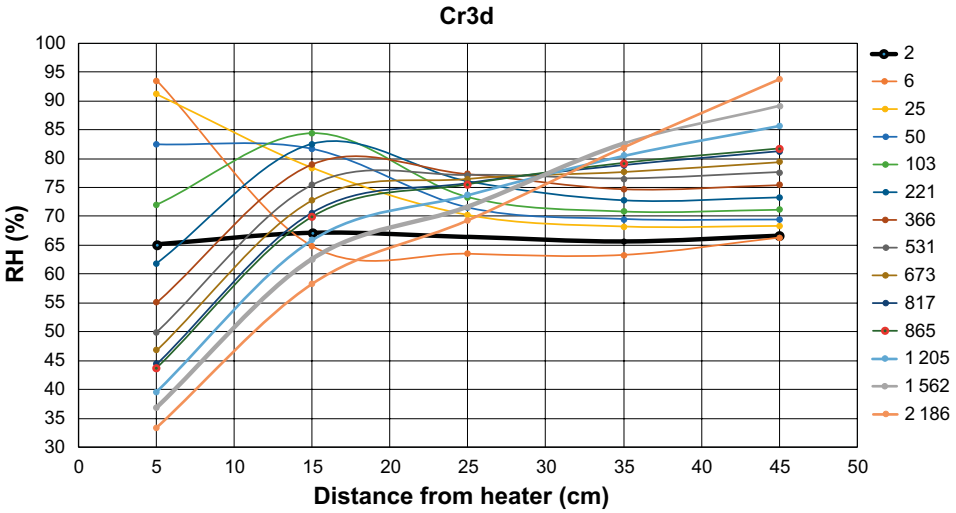

Figure 4-16. *RH profiles at different times (hours) in test Cr3d.*

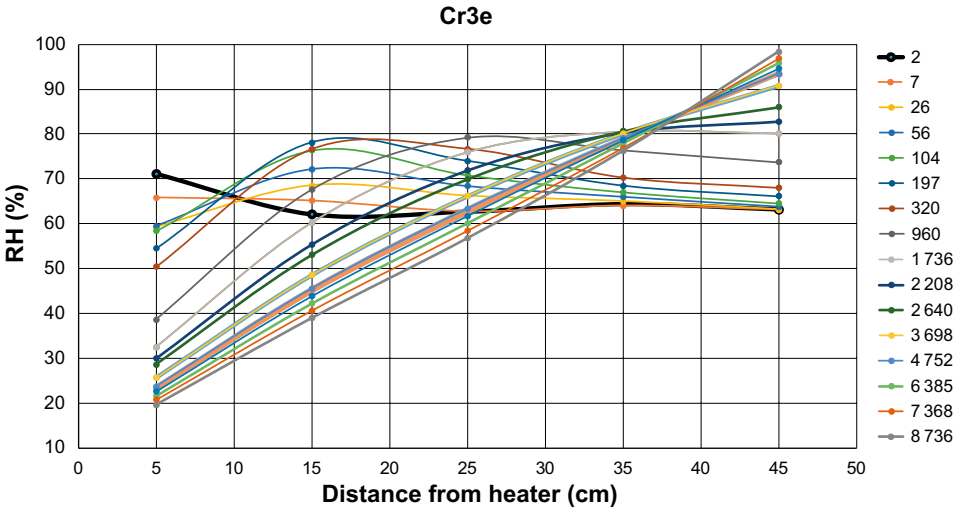

Figure 4-17. *RH profiles at different times (hours) in test Cr3e.*

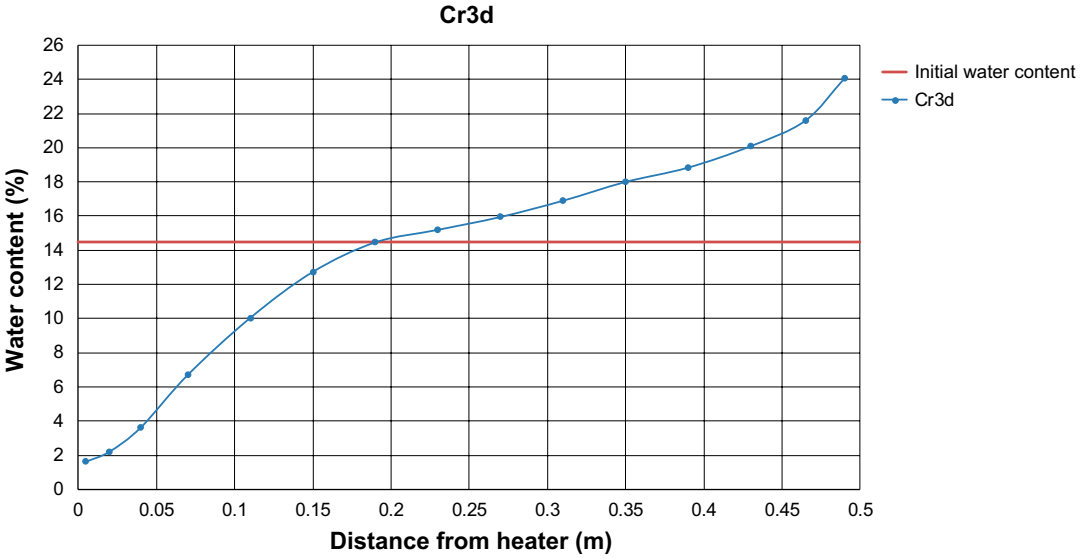

Figure 4-18. *Water content profile at the end of test Cr3d (2 186 hours).*

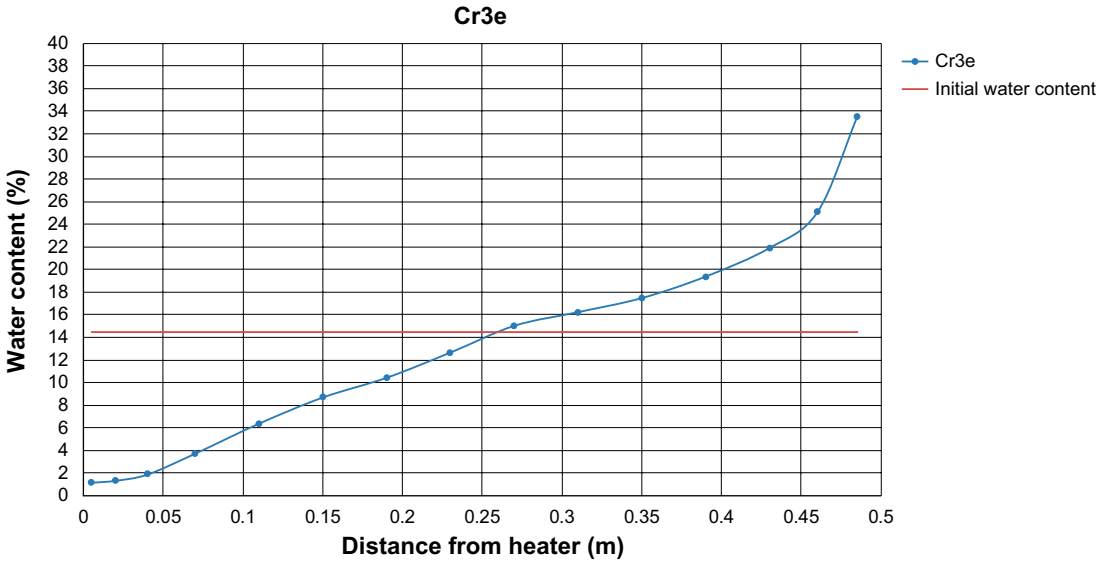

Figure 4-19. Water content profile at the end of test Cr3e (8 736 hours).

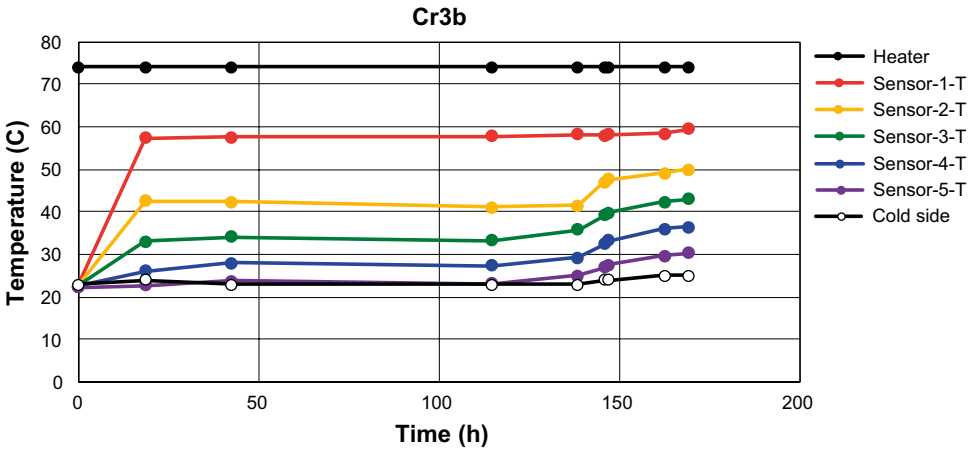

Figure 4-20. Temperature evolution at sensor positions, heater and cold end in test Cr3b.

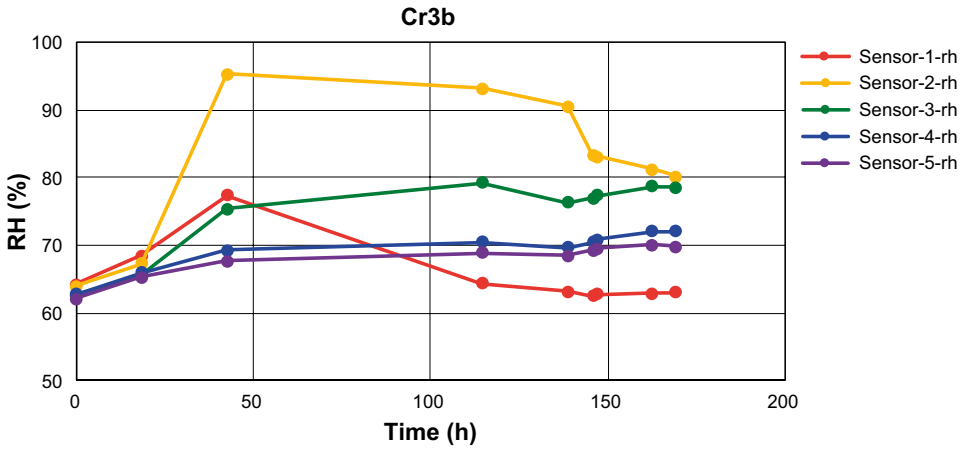

Figure 4-21. RH evolution at sensor positions in test Cr3b.

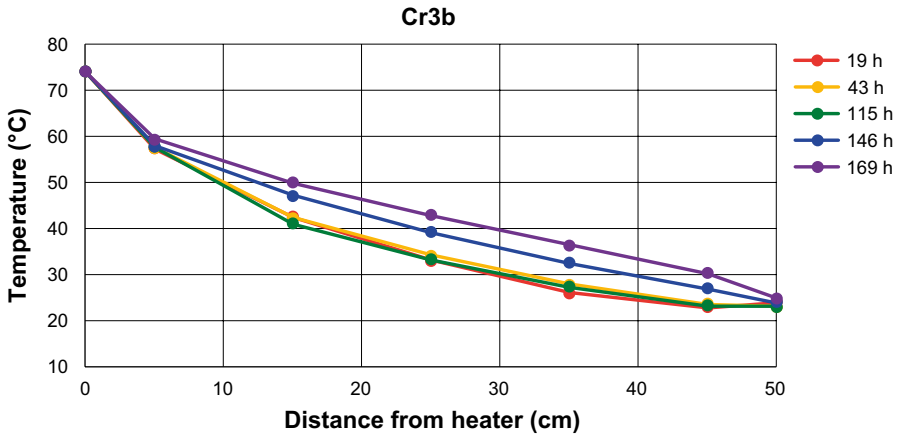

Figure 4-22. *Temperature profiles at different times (hours) in test Cr3b.*

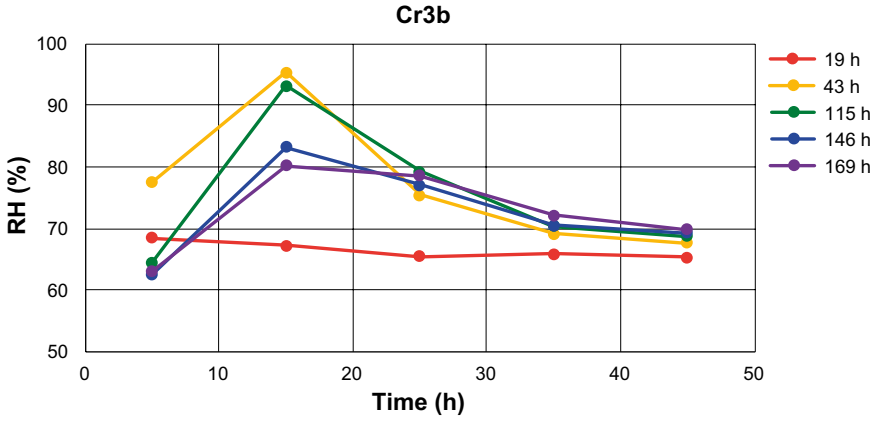

Figure 4-23. *RH profiles at different times (hours) in test Cr3b.*

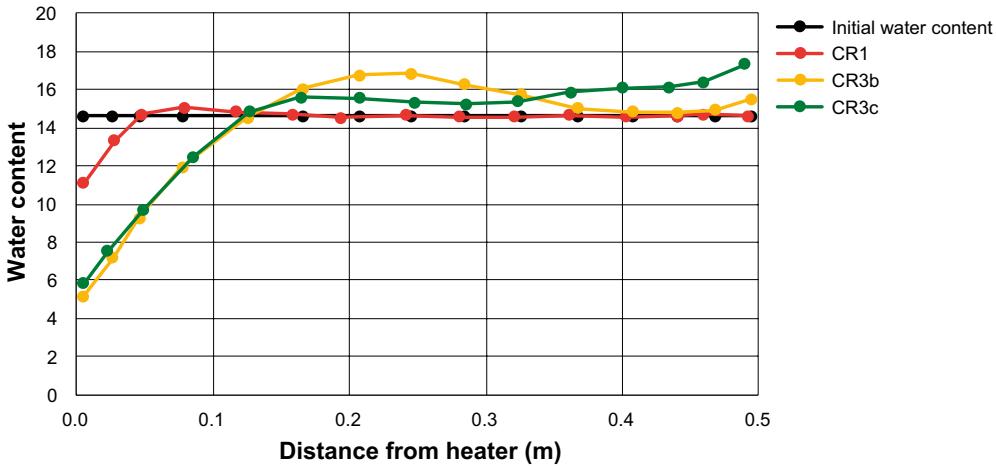

Figure 4-24. *Water content profiles at the end of test for Cr1, Cr3b Cr3c. The results of tests Cr1 and Cr3c are uncertain.*

4.3 Discussion

Temperature evolution and profiles

The temperature profiles shown in Figure 4-14 and Figure 4-15 demonstrate that steady-state conditions were reached during the first day (Cr3d) or during the first two days (Cr3e) in the long-term tests with roller-compacted MX-80 pellets. This delay was caused by a modification of the thermal insulation made after one day. The profiles show that the temperature levels reached in the Cr3e test were higher than in Cr3d. The difference was approximately 5 °C higher at the warmest sensor position. This difference shows that the improved thermal insulation had the desired effect. After steady-state conditions were reached, there were no noticeable changes in the temperature profiles. This implies that there wasn´t any noticeable change in thermal conductivity, even though the moisture content was significantly redistributed. The thermal gradient close to the heater in both tests, especially in Cr3d, was however distinctly higher than in the remaining part of the test tube, which indicated that some heat was lost through the insulation. The temperature evolution in the test with extruded Asha pellets (Ce3d) displayed some minor irregular trends during the first 25 days (Figure 4-5) and stable steady-state conditions were not reached until after that time period (Figure 4-7).

The temperature control of the warm side was controlled with a PT100 sensor located on (Cr3d) or inside (Cr3e) the bottom plate and with a control unit which turned on the heating plate at a temperature of 72.8 °C and turned it off at 73.0 °C. Due to the inertia of the system this implied that the temperature measured with the PT100 varied between 72.8 °C and approximately 78 °C with a periodicity of approximately 17 minutes. This implies that the average temperature inside (or on) the bottom plate was ~75.5 °C, i.e. 1.5 °C higher than the defined target value for the boundary.

RH evolution and profiles

The RH values in test Cr3d evolved from an initial level of 66–67 % to a final profile ranging from 33 to 94 %. Corresponding initial level for test Cr3e was 63–65 %, while the final profile ranged from 20 to 98 %. The initial behaviour of the two tests was slightly different: the initial RH at the warmest sensor position was higher in the Cr3d test and the time to reach the final order of precedence (with decreasing RH for increasing temperature) was shorter in the Cr3d test. The RH data for the Cr3d test did not level out before the end of the test which showed that steady-state wasn´t reached during the test period. The data for the Cr3e also displayed some diverging trends (although significantly smaller) after one year. The RH-evolution in the test with extruded Asha pellets (Ce3d) started from an initial level of 51–52 % and displayed a final profile ranging from 28 to 81 %.

Water content profiles

The results show that a significant moisture redistribution took place during the test period. The water content in test Cr3d diverged from 14.5 % to a final profile ranging from 1.6 to 24 %. The corresponding initial level for test Cr3e was also 14.5 %, while the final profile ranged from 1.2 to 34 %. The test with extruded Asha pellets (Ce3d) started from an initial water content of 14.7 % and displayed a final profile which ranged from 4.1 to 20.5 %.

Estimation of displacements

The displacement during the tests period of test Cr3e was estimated through photography of the lateral surface of the test tube together with a yard stick placed in the same position, prior and subsequent to the tests period. By studying pairs of photographs, taken approximately perpendicular to the test tube and at the same level, and by measuring the levels of common features in the two photographs, an estimate of the displacement field could be obtained (Figure 4-25). The maximum displacement value was 15 mm.

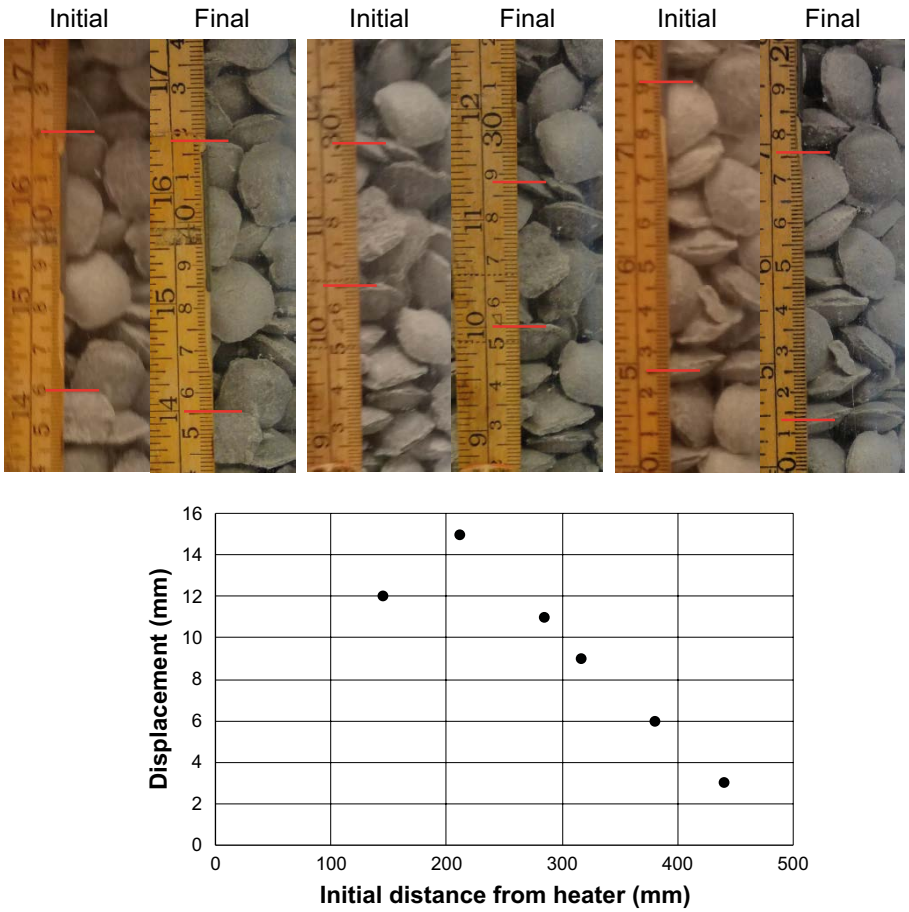

Figure 4-25. *Estimated displacement directed towards the warm end (lower). Values evaluated from yard stick readings in pairs of photographs, taken prior and subsequent to the test period, in which common features could be identified. The initial distance from heater is the initial yardstick reading plus 20 mm (i.e. the thickness of the lower flange of the Plexiglas tube).*

Consistency of different data sets

Three evaluation of the consistency of different data sets are presented below regarding: i) the initial and the final water content profiles; ii) the water content and the RH; and iii) the vapour pressure evolution.

The initial and final water content profiles were compared by calculating the relative error between the initial and final length integral of the water content:

$$Relative\ error = \frac{\sum w_i \cdot l_i - w^{init} \cdot L}{w^{init} \cdot L} \qquad (4\text{-}1)$$

where L is the length of the equipment, w^{init} is the initial water content, and w_i and l_i are the water content and the length, respectively, of each sample i. A compilation of calculated water content integrals for the Cr3d, Cr3e and Ce3d tests are shown in Table 4-3. It can be noted that there appears to be a general loss of water, but that the relative error was small.

Table 4-3. Relative error between initial and final water content.

Test	$\Sigma w_i \cdot l_i$ (%·m)	$w^{init} \cdot L$ (%·m)	Rel. error (%)
Cr3d	7.21	7.25	−0.5
Cr3e	6.85	7.25	−5.5
Ce3d	7.04	7.35	−4.2

The accuracy of the RH sensors was investigated through analysis of the consistency between the *final RH values and the final water content profile*. This relation was compared with independently determined water retention curves for two different initial water contents: 17 % (Dueck 2004) and 10 % (Dueck and Nilsson 2010); both by comparing water content versus RH, and by comparing water content versus suction, thereby taking the different temperature levels into account (Figure 4-26). It was found that the data from Cr3e was generally consistent with the water retention curves, especially when the temperature was considered. The RH sensor at the coolest position was however an exception and showed 98 %, although a value of 93–94 % would be more in agreement with the final water content. This observation was supported by the results from tests performed after the dismantling, in which the sensors were placed inside a climate chamber during periods with specified RH levels. These tests showed that the sensor at the warmest (and driest) position displayed quite accurate results, whereas the sensor at the coolest (and most humid) position displayed results which were approximately 4 % units too high. The deviation of the sensors positioned between these extremes was quite linear.

The accuracy of the RH sensors was further investigated through analysis of the *vapour pressure evolution.* This was calculated as the product of the measured RH and the saturated vapour pressure, which in turn was calculated from the measured temperate (T):

$$p_v^{sat}(T) = 136075 \cdot \exp\left(\frac{-5239.7}{273.15 + T}\right) \quad (MPa) \tag{4-2}$$

(Gens et al. 2009). The evaluated evolution of the vapour pressure for the five sensors in test Cr3e is show in Figure 4-27. It can be noted that the trends are realistic in the sense that the values for the different sensors tend to converge and that the curves at no point tended to cross each other.

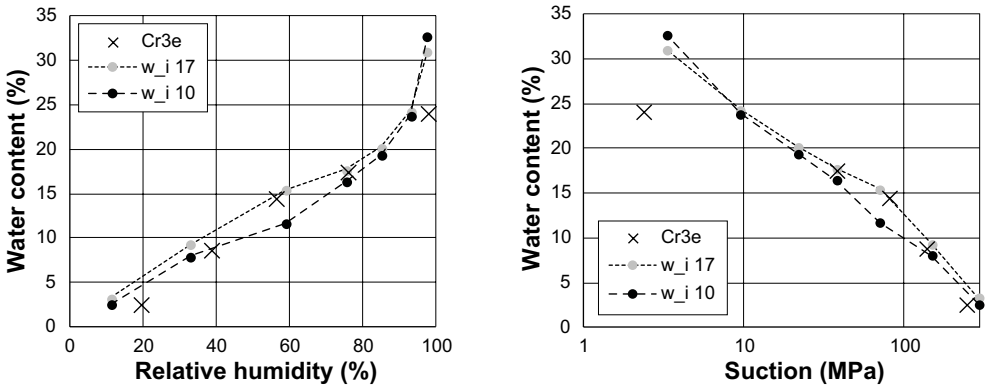

Figure 4-26. *Relation between final RH readings and water contents representative for the sensor positions (left). Corresponding comparison for suction versus water content (right). Data points compared with two sets of water retention curves for initial water content of 17 and 10 %.*

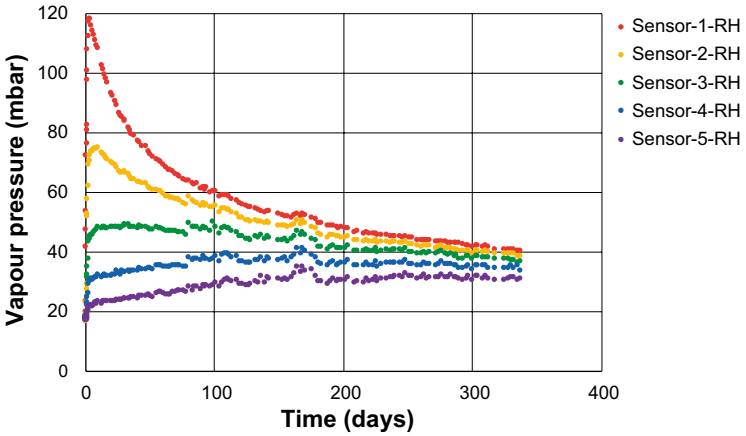

Figure 4-27. *Evaluated vapour pressure evolution for the five sensors in test Cr3e.*

Method development

As with the type A tests, the length of the used test equipment has implied very long test times. And a shorter length would therefore imply that more information about the investigated processes would be gained within a certain time frame.

Moreover, the measured temperature profiles indicate that the type C tests were influenced by a significant thermal leakage through the lateral surface. The magnitude of such a leakage could be reduced by increasing the ratio between the diameter and the length of the test equipment.

The potential influence of gravity and natural convection could also be investigated if the orientation of the test setup could be turned 90° which would mean that the temperature gradient would be perpendicular to the gravity vector.

5 Modelling task and subtasks

5.1 Task description – Subtask A

The goal of Subtask A was to model the type A tests for the two pellet types. The following results were requested:

- Water consumption as a function of time.
- RH evolution in the measuring points.
- Water content as function of distance from bottom at the three times at test termination.
- Dry density and degree of saturation as function of distance from bottom at the three times at test termination (if modelled).
- Additional relevant information and results.

5.2 Task description – Subtask C

The goal of Subtask C was to model the type C tests for the two pellet types. The following results were requested:

- RH evolution in the measuring points.
- Water content distribution at the times when the tests were terminated.
- Temperature evolution in the measuring points (applied or modelled).
- Distribution of dry density and degree of saturation at the times when the tests were terminated (if modelled).
- Additional relevant results and information.

It was recommended that the measured temperature evolution would be used as input to the models.

5.3 Requested results

The scope of the modelling task was focused by requesting results from at least four cases which represented the two subtasks and the two materials. These cases corresponded to the regular long-term water-uptake tests (Ae3 and Ar3), and the thermal gradient tests with the longest duration (Ce3d and Cr3e). The set of experimental data from these tests thereby specified the main part of the requested model results (Table 5-1). Water content profiles from tests with shorter duration (Ae1, Ae2, Ar1, Ar2 and Cr3d) were regarded as representative for the intermediate conditions for three of the model cases.

Table 5-1. Specification of requested results for the different subtasks and materials.

Pellets	Subtask A	Subtask C
Asha	● **Water content vs distance** (0, 5, 30 & 200 days) ● **Water uptake vs time** (0–200 days)	● **RH vs time** (0–90 day; 5, 15, 25, 35 & 45 cm) ● **Temp vs time** (0–90 days; 5, 15, 25, 35 & 45 cm) ● **Water content vs distance** (0 & 90 days)
MX-80	● **Water content vs distance** (0, 5, 30 & 200 days) ● **Water uptake vs time** (0–200 days) ● **RH vs time** (0–200 day; 3, 8, 15.5 cm)	● **RH vs time** (0–365 days; 5, 15, 25, 35 & 45 cm) ● **Temp vs time** (0–365 days; 5, 15, 25, 35 & 45 cm) ● **Water content vs distance** (0, 90, 365 days)

6 Air permeability tests

The air flow resistance through pellet fillings has been investigated in a number of tests performed on the two pellet types. Figure 6-1 shows the equipment. A Plexiglas tube of the same dimension as used for the other tests was filled with bentonite pellets. In the bottom of the tube a perforated delimiter was placed in order to keep the pellets in place but not affect the air flow through the pellets. The same type of Plexiglas tube was placed under the delimiter. The lower tube was connected to an air pump equipped with a flow meter. A differential pressure transducer was placed in the tube.

The tests were done by upholding a constant air pressure in the lower tube and measure the air flow rate. Tests were only done on the MX-80 roller compacted pellets. Two bulk densities were tested.

$\rho_d = 915$ kg/m^3

$\rho_d = 997$ kg/m^3

The higher density was achieved by shaking the tube. A number of tests with different air pressure were conducted. Figure 6-2 shows the results.

Figure 6-1. *Test set up for the air permeability tests.*

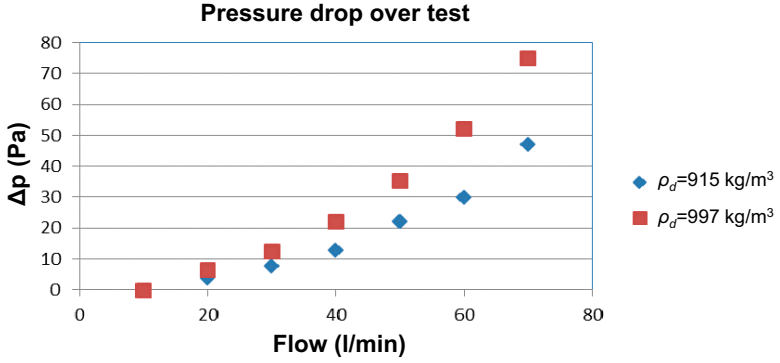

Figure 6-2. *Results of the air permeability tests on MX-80 roller compacted pellets.*

7 Concluding remarks

The presented tests have resulted in data sets which are well suited for the adoption and development of material models for bentonite pellets.

In general, the different data sets appear to display a high level of consistency. For the A tests, this was noted regarding: i) the water content data and the RH data; and ii) the initial water uptake and the boundary pressure. For the C tests a corresponding consistency was found regarding: i) the initial and final water content profiles; ii) the water content data and the RH data; and iii) the vapour pressure evolution. The measured cumulative water uptake in the A tests were however significantly larger than the calculated water uptake implied from the measured water content profiles. The most likely cause for this deviation was that the measured water uptake data was influenced by different types of evaporation and leakage.

Acknowledgement

This experimental work for tests Cr3d and Cr3e was jointly funded by Radioactive Waste Management (RWM) and SKB. All other work was funded by SKB.

References

SKB's (Svensk Kärnbränslehantering AB) publications can be found at www.skb.com/publications.

Andersson L, Sandén T, 2012. Optimization of backfill pellets properties. ÅSKAR DP2. Laboratory tests. SKB R-12-18, Svensk Kärnbränslehantering AB.

Börgesson L, Sandén T, Dueck A, Andersson L, Jensen V, Nilsson U, Olsson S, Åkesson M, Kristensson O, Svensson U, 2015. Consequences of water inflow and early water uptake in deposition holes. EVA project. SKB TR-14-22, Svensk Kärnbränslehantering AB.

Dueck A, 2004. Hydro-mechanical properties of a water unsaturated sodium bentonite: laboratory study and theoretical interpretation. PhD thesis. Lund University, Sweden.

Dueck A, Nilsson U, 2010. Thermo-hydro-mechanical properties of MX-80. Results from advanced laboratory tests. SKB TR-10-55. Svensk Kärnbränslehantering AB.

Fransson Å, Åkesson M, Andersson L, 2017. Bentonite Rock Interaction Experiment. Characterization of rock and installation, hydration and dismantling of bentonite parcels. SKB R-14-11, Svensk Kärnbränslehantering AB.

Gens A, Sánchez M, Guimarães L D N, Alonso E E, Lloret A, Olivella S, Villar M V, Huertas F, 2009. A full-scale in situ heating test for high-level nuclear waste disposal: observations, analysis and interpretation. Géotechnique 59, 377–399.

Johannesson L-E, Sandén T, Dueck A, 2008. Deep repository – engineered barrier system. Wetting and homogenization processes in backfill materials. Laboratory tests for evaluation modeling parameters. SKB R-08-136, Svensk Kärnbränslehantering AB.

Sandén T, Jensen V, 2016. Pellet optimization – influence of fines. KBP1011 Water handling during backfill installation. SKB R-16-15, Svensk Kärnbränslehantering AB.

Sandén T, Olsson S, Andersson L, Dueck A, Jensen V, Hansen E, Johnson A, 2014. Investigation of backfill candidate materials. SKB R-13-08, Svensk Kärnbränslehantering AB.

Sandén T, Nilsson U, Andersson L, 2016. Investigation of parameters influencing the bentonite block quality. Laboratory investigation. SKB P-16-06, Svensk Kärnbränslehantering AB.

Sellin P (ed), Åkesson M, Kristensson O, Malmberg D, Börgesson L, Birgersson M, Dueck A, Karnland O, Hernelind J, 2017. Long re-saturation phase of a final repository. Additional supplementary information. SKB TR-17-15, Svensk Kärnbränslehantering AB.

Arkitektkopia AB, Bromma, 2020

SKB is responsible for managing spent nuclear fuel and radioactive waste produced by the Swedish nuclear power plants such that man and the environment are protected in the near and distant future.

skb.se